Plant, Cell and Environment (2006) **29**, 928–939 doi: 10.1111/j.1365-3040.2005.01474.x

Non-steady state effects in diurnal ^{18}O discrimination by *Picea sitchensis* branches in the field

U. SEIBT[1,2*], L. WINGATE[3*], J. A. BERRY[2] & J. LLOYD[1†]

[1]*Max Planck Institute for Biogeochemistry, Jena, Germany,* [2]*Department of Global Ecology, Carnegie Institution of Washington, Stanford, CA, USA and* [3]*School of GeoSciences, University of Edinburgh, Edinburgh, UK*

ABSTRACT

We report diurnal variations in ^{18}O discrimination ($^{18}\Delta$) during photosynthesis ($^{18}\Delta_A$) and respiration ($^{18}\Delta_R$) of *Picea sitchensis* branches measured in branch chambers in the field. These observations were compared with predicted $^{18}\Delta$ ($^{18}\Delta_{pred}$) based on concurrent measurements of branch gas exchange to evaluate steady state and non-steady state (NSS) models of foliage water ^{18}O enrichment for predicting the impact of this ecosystem on the $\delta^{18}O$ of atmospheric CO_2. The non-steady state approach substantially improved the agreement between $^{18}\Delta_{pred}$ and observed $^{18}\Delta$ ($^{18}\Delta_{obs}$) compared with the assumption of isotopic steady state (ISS) for the $\delta^{18}O$ signature of foliage water. In addition, we found direct observational evidence for NSS effects: extremely high apparent $^{18}\Delta$ values at dusk, dawn and during nocturnal respiration. Our experiments also show the importance of bidirectional foliage gas exchange at night (isotopic equilibration in addition to the net flux). Taken together, neglecting these effects leads to an underestimation of daily net canopy isofluxes from this forest by up to 30%. We expect NSS effects to be most pronounced in species with high specific leaf water content such as conifers and when stomata are open at night or when there is high relative humidity, and we suggest modifications to ecosystem and global models of $\delta^{18}O$ of CO_2.

Key-words: branch chamber method; leaf water enrichment; nocturnal stomatal conductance.

INTRODUCTION

The $^{18}O/^{16}O$ ratio of atmospheric CO_2 has been used as an independent tracer of carbon and water fluxes in modelling and field studies at the ecosystem (Yakir & Wang 1996; Riley *et al*. 2002; Bowling *et al*. 2003) and at the global scale (Francey & Tans 1987; Ciais *et al*. 1997a, b; Cuntz *et al*. 2003a, b). Such studies require accurate models of ^{18}O fractionations during photosynthesis and respiration. The theory of this has been developed (Farquhar & Lloyd 1993) and tested in the laboratory for photosynthesis (e.g. Farquhar *et al*. 1993; Gillon & Yakir 2000) and recently for respiration (Cernusak *et al*. 2004). But few studies on the range of ^{18}O discrimination ($^{18}\Delta$) under field conditions have been published (Harwood *et al*. 1998; Wang, Yakir & Avishai 1998; Seibt 2003). Consequently, the natural variability of $^{18}\Delta$ is largely unknown.

The enrichment or depletion of ^{18}O in ambient CO_2 during photosynthesis and respiration is dominated by the isotopic exchange of CO_2 and water during interconversion between CO_2 and H_2CO_3. The reaction is catalysed by the enzyme carbonic anhydrase and is thus very fast in leaves (Francey & Tans 1987), but slow in environmental water. As CO_2 can enter and diffuse back out of the foliage (retrodiffusion) without being assimilated, its $\delta^{18}O$ signature will reflect nearly complete isotopic equilibration with the water it contacts in the leaf. The magnitude of ^{18}O fractionation during CO_2 exchange between foliage and canopy air thus depends on the isotopic signature of water close to the evaporation sites. Because the $\delta^{18}O$ value of foliage water at these evaporating sites, $\delta^{18}O_E$, is transferred to atmospheric CO_2 (Farquhar *et al*. 1993), it is important to test how well the existing models predict the ^{18}O enrichment of foliage water under field conditions over the diurnal cycle.

During foliage transpiration, the lighter isotope diffuses faster than the heavier one, thereby enriching the water at the evaporating sites in ^{18}O. The extent of ^{18}O enrichment is controlled by the bidirectional exchange of water vapour between the foliage surface and air, and is thus inversely proportional to relative humidity in the surrounding air. In the steady state description, the value of $\delta^{18}O_E$ instantly adjusts to any change in environmental conditions. The steady state enrichment model (Craig & Gordon 1965) is widely used to predict $\delta^{18}O_E$ in modelling studies at ecosystem and global scales (e.g. Farquhar *et al*. 1993; Ciais *et al*. 1997a, Ometto *et al*. 2005). The basic assumption of this model, that foliage water is at isotopic steady state (ISS), however, is not necessarily fulfilled at all times, especially under field conditions (Bariac *et al*. 1994; Harwood *et al*. 1998; Cernusak, Pate & Farquhar 2002). Dongmann *et al*. (1974) developed a non-steady state (NSS) version of the enrichment equation, incorporating the finite turnover of the foliage water pool. In this approach, the time necessary for foliage water to attain an ISS is determined by the

*Correspondence: Ulrike Seibt. Fax: +1-650-462-5968; e-mail: useibt@ stanford.edu

**These authors contributed equally to the work.*
†*Present address: School of Geography, University of Leeds, Leeds, UK.*

rate of bidirectional exchange of water vapour relative to the water content of the foliage. Cernusak *et al*. (2002) applied such an NSS model to measurements of phloem sap and leaf water $\delta^{18}O$ values and found good agreement between the predicted and observed time courses of $\delta^{18}O$ signatures. The NSS model was recently modified to additionally include variations in the foliage water volume (Cernusak, Farqukar & Pate 2005; Farquhar & Cernusak 2005).

Here, we explore the effects of the NSS enrichment of evaporating site water on the $\delta^{18}O$ signatures of CO_2 exchanged between foliage and canopy air under field conditions. We report on diurnal variations in ^{18}O fractionation occuring during photosynthesis and respiration in a stand of Sitka spruce (*Picea sitchensis*) growing in Central Scotland. The method we applied combines the analysis of air samples collected from branch chambers with measurements of environmental variables and gas exchange in the chambers, representing well-defined, enclosed subspaces within the forest canopy. This approach enabled us to investigate concurrent processes simultaneously. From the chamber measurements of microclimate and gas exchange, we predicted the $\delta^{18}O$ signatures of photosynthetic and respiratory CO_2 fluxes on the basis of the steady state and NSS assumptions. We then compared these predictions with the observed $\delta^{18}O$ signatures of CO_2 from the chamber air samples.

MATERIALS AND METHODS

Study site and gas exchange measurements

The study was conducted in Griffin Forest, a plantation of Sitka Spruce (*P. sitchensis*) located near Aberfeldy, Perthshire, UK (56°37′N, 3°48′W). Wingate (2003) gives a detailed description of the experimental set-up. Branch chambers were installed in the upper canopy at 10.5 and 9.4 m (chambers 1 and 3, respectively), and in the middle canopy at 8.1 m (chamber 4). The latter was used as a control (empty) chamber in July 2001. The chambers were operated on an automated 20 min cycle. Each chamber was open and ventilated for 15 min, after which it was closed for 5 min, and the CO_2 mole fraction, relative humidity, photon flux density and temperatures inside were monitored. From these data, rates of net CO_2 assimilation (A), stomatal conductance to water vapour (g_s), and the leaf surface, intercellular and chloroplast CO_2 mole fractions (C_s, C_i, and C_c) were calculated at each 20 min time step for the beginning as well as over the full closure period (see Appendix b for details of the gas exchange calculations).

Collection and analysis of water samples

Needle and non-green twig samples were collected from the same or adjacent Sitka spruce trees. The samples were taken at the same heights and close (≈ 2 m) to the chamber locations. Soil samples were collected in the vicinity of the trees from the top 5 cm of the soil below the litter layer. In the field, all samples were placed in a cooler in sealed glass containers. These were then transferred to a freezer in the lab and stored until further processing. Water was extracted from the samples cryogenically under vacuum and was collected in small glass vials to which a known amount of CO_2 was added. Vials were then left for a minimum of 3 d to allow CO_2–H_2O equilibration. The $\delta^{18}O$ of the equilibrated CO_2 was measured on a dual inlet isotope ratio mass spectrometer. The overall precision for water $\delta^{18}O$ data was 0.4‰. All water $\delta^{18}O$ values are reported with respect to Vienna Standard Mean Ocean Water (VSMOW). Extractions and analyses were performed at the University of Cambridge, UK and at the Weizman Institute of Science, Rehovot, Israel.

Collection and analysis of flask air samples

Pairs of air samples from branch chambers were collected at intervals of approximately 3 h over 24 h in spring (18/19 May) and summer (20 July) 2001. Air was circulated from the branch chambers through sampling lines into a flask sampling system (separate from that used for gas exchange measurements) and back into the chamber. Within the sampling system, the air stream was passed through a magnesium perchlorate cylinder to remove water vapour and was pumped through two flasks in series. We used 1 dm^3 glass flasks with a valve (Glass Expansion, Melbourne, Australia) on each end, sealed with Teflon® perfluoroalkoxy (PFA) O-rings (Du Pont Fluoroproducts, Wilmington, DE, USA) and 1.3 dm^3 flasks with two valves (Louwers, Hapert, Netherlands) on the same end. Flask samples were taken at two points in the opening and closing sequence of branch chambers. The first flask was collected 3–4 min before closure ('open sample') and reflects the CO_2 mole fraction and isotopic signature of ambient canopy air. The second flask ('closed sample') was collected shortly before reopening of the chamber.

All flasks were analysed at the Max Planck Institut (MPI) für Biogeochemie in Jena, Germany. The CO_2 mole fractions in the air samples were determined using a gas chromatograph (HP 6890, Hewlett Packard, CA, USA) linked to a methanizer and flame ionization detector. The CO_2 in the dry air samples was then extracted cryogenically ('BGC-AirTrap', Werner, Rothe & Brand 2001), and its isotope ratio was determined on a dual inlet isotope ratio mass spectrometer (Delta$^+$XL, Finnigan MAT, Bremen, Germany). The analytical precision was in the order of 0.08 μmol mol^{-1} for CO_2 mole fraction and 0.02‰ for $\delta^{18}O$, reported with respect to Vienna-Pee Dee Belemnite (V-PDB)-CO_2. The uncertainties of flask data were estimated from the SDs of the laboratory analysis of duplicate flasks, 0.13 μmol mol^{-1} for CO_2 mole fraction and 0.03‰ for $\delta^{18}O$. Additional uncertainties arising from the sampling procedure, applying to samples collected at the end of closure periods, were estimated from control measurements in an empty chamber. They were 1.3 μmol mol^{-1} for CO_2 mole fraction and 0.2‰ for $\delta^{18}O$.

Calculation of $\delta^{18}O$ signatures of CO_2 exchange from flask data

In analogy to a Rayleigh process, the observed values of $^{18}\Delta$ during photosynthesis [$^{18}\Delta_{A,obs}$ (‰)] and nocturnal respiration [$^{18}\Delta_{R,obs}$ (‰)] of foliage in the closed branch chamber were determined after Guy *et al*. (1989):

$$^{18}\Delta_{A,obs/R,obs} = -\frac{\ln(R_e/R_o)}{\ln(C_e/C_o)}\left[1+\frac{\ln(R_e/R_o)}{\ln(C_e/C_o)}\right]^{-1}, \quad (1)$$

where C_o and C_e are the mole fractions (μmol mol^{-1}), and R_o and R_e are the $^{18}O/^{16}O$ ratios of CO_2 at the beginning and at the end of the closure periods, respectively. These correspond to the samples collected from the open and closed chambers for flask measurements, and to the starting time values and those integrated over the closure periods for gas exchange data (Appendix B). The above definition relates isotopic exchanges to the net exchange of CO_2, but note that a large part of the apparent discrimination is associated with isotopic equilibration of CO_2 which can occur in the absence of net exchange. This equation can therefore yield large apparent observed $^{18}\Delta$ ($^{18}\Delta_{obs}$) at times of small net CO_2 fluxes. Estimated uncertainties for $^{18}\Delta_{obs}$ were calculated using Gaussian error propagation. They were inversely related to net flux rates, usually < 2‰, but > 10‰ at night, dawn and dusk. Discrimination values were also very large at these times.

All calculations were performed in Interactive Data Language (IDL version 6.1, Research Systems Inc., Boulder, CO, USA). Correlation parameters between predicted $^{18}\Delta$ ($^{18}\Delta_{pred}$) and $^{18}\Delta_{obs}$ were obtained from least absolute deviation regressions using the flask observations as independent variable. Night-time data points were excluded because of the limited number of conductance measurements at night. Four day-time data points were also excluded because of lack of reliable gas exchange measurements [18 May, 0710, infrared gas analyser (IRGA) tubing detached; 0740, relative humidity constant at 50%; 1740, sensor artefacts from direct sunlight; 20 July, 0340, air saturated].

Theory

The $\delta^{18}O$ signature of foliage CO_2 exchange

Assuming full isotopic equilibrium with foliage water, $^{18}\Delta$ during photosynthesis [$^{18}\Delta_A$ (‰)] and nocturnal respiration [$^{18}\Delta_{R,bi}$ (‰, bi stands for bidirectional foliage gas exchange)] can be written to reasonable approximation (Farquhar *et al*. 1993; Farquhar & Lloyd 1993; Cernusak *et al*. 2004) as

$$^{18}\Delta_{A/R,bi} = \bar{a} + (\delta^{18}O_{c-eq} - \delta^{18}O_a)\frac{C_c}{C_a - C_c}, \quad (2)$$

where C_a, $\delta^{18}O_a$ and C_c, $\delta^{18}O_{c-eq}$ are the mole fractions and isotopic compositions of CO_2 in ambient air and at the site of isotopic equilibration, respectively. The offset between the equilibrated CO_2 ($\delta^{18}O_{c-eq}$) and foliage water ($\delta^{18}O_{cw}$) depends on leaf temperature T (K) as $\varepsilon_{c-eq} = 17\,604/T - 17.93$ (Brenninkmeijer, Kraft & Mook 1983). In the following, we assumed that the isotopic exchange is limited to the chloroplasts (C_c), that the $\delta^{18}O_E$ of evaporating site water is a good approximation for $\delta^{18}O_{cw}$ (Farquhar & Lloyd 1993; Cernusak *et al*. 2004) and that the isotopic exchange is complete (i.e. $\theta = 1$, Gillon & Yakir 2000). The fractionation coefficient for diffusion of CO_2 to the sites of isotopic exchange, $\bar{a}$, expresses the mean of the successive diffusion steps through leaf boundary layer (5.8‰), stomata (8.8‰) and the liquid phase (0.8‰), weighted by the CO_2 drawdown associated with each step (Farquhar & Lloyd 1993). The boundary layer conductance was estimated from temperature, light and water flux data (1.5 ± 0.5 mol m^{-2} s^{-1}). The mesophyll conductance required for $\bar{a}$ and C_c was estimated from concurrent $^{13}\Delta_{obs}$ data (0.16 mol m^{-2} s^{-1}, see Seibt 2003; Wingate 2003). The calculation of $^{18}\Delta$ from chamber data during flask sampling periods is detailed in Appendix B.

Equations 1 and 2 relate the $^{18}\Delta$ signature to net CO_2 exchange. If isotopic exchange occurs without any net CO_2 flux, neither of the two descriptions can be applied. For comparison, the isotopic signatures of nocturnal foliage respiration using the (now obsolete) net-flux description ($\delta^{18}O_{R,net}$), corresponding to Eqn 2 for the case where $C_c >> C_a$, were also expressed as $^{18}\Delta$ values, $^{18}\Delta_{R,net}$ (‰):

$$^{18}\Delta_{R,net} = \bar{a} - \delta^{18}O_{c-eq} + \delta^{18}O_a \quad (3)$$

The $\delta^{18}O$ signature of water at the evaporating sites of foliage

The $\delta^{18}O_E$ value of evaporating site foliage water assuming steady state conditions, $\delta^{18}O_{ISS}$, can be calculated using the Craig-Gordon model (Craig & Gordon 1965; Dongmann *et al*. 1974; Farquhar *et al*. 1993):

$$\delta^{18}O_{ISS} = \delta^{18}O_s + \varepsilon_k + \varepsilon_{eq} + (\delta^{18}O_v - \delta^{18}O_s - \varepsilon_k)\frac{w_a}{w_i}, \quad (4)$$

where w_a/w_i is the ratio of ambient to leaf intercellular vapour mole fraction, and $\delta^{18}O_S$ and $\delta^{18}O_V$ are the $\delta^{18}O$ signatures of source water and canopy water vapour. The equilibrium fractionation for the liquid to vapour phase transition was calculated from leaf temperature T (K) as $\varepsilon_{eq} = \exp(1137/T^2 - 0.4156/T - 0.0020667)$ (Majoube 1971). The kinetic fractionation, ε_k, was derived from the isotope effects during water vapour diffusion through the stomata and boundary layer (Farquhar *et al*. 1993) as $\varepsilon_k = (32r_s + 21r_b)/(r_s + r_b)$, where r_s and r_b are the stomatal and boundary layer resistances to diffusion of water vapour, and 32 and 21‰ are their respective fractionation coefficients (Cappa *et al*. 2003). The simplified expression in Eqn 4 underestimates $\delta^{18}O_{ISS}$ by ≈ 0.1‰, usually negligible compared with experimental uncertainties (Farquhar & Lloyd 1993; Cernusak, Wong & Farquhar 2003).

The expression for the NSS isotopic composition of evaporating site water, $\delta^{18}O_{NSS}$, follows the time course of the leaf water isotopic composition towards an ISS (Dongmann *et al*. 1974):

$$\delta^{18}O_{NSS}(t) = \delta^{18}O_{ISS}(t) - [\delta^{18}O_{ISS}(t) - \delta^{18}O_{NSS}(t-\Delta t)] \cdot e^{\left(-(1-\varepsilon_k)(1-\varepsilon_{eq})\frac{\Delta t}{\tau}\right)}, \quad (5)$$

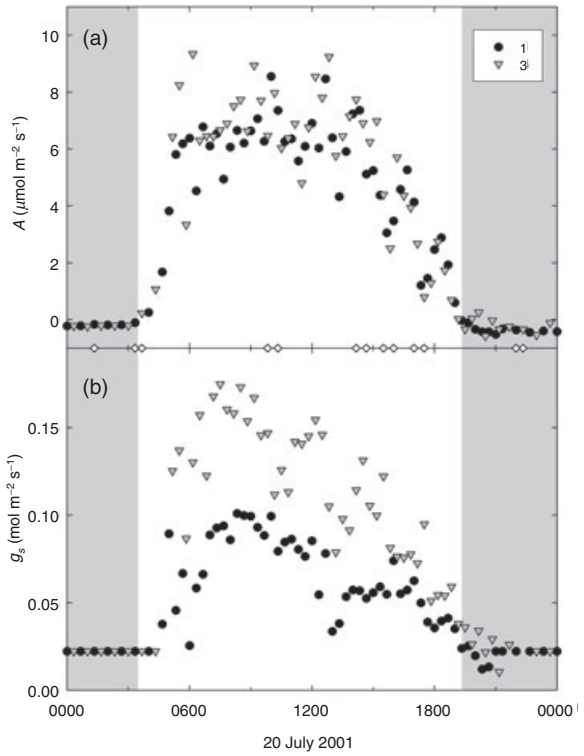

Figure 1. Diurnal variation in measured (a) net CO_2 assimilation rates, A (b) stomatal conductance to water vapour (g_s), for foliage in the upper branch chambers (1, ●; 3, ▼) on 20 July 2001. The symbols on the time axis between the two panels (◇) indicate the times when flask samples were collected. The grey areas in Figs 1–4 mark the approximate times of observed net respiratory fluxes of CO_2.

where $\delta^{18}O_{ISS}(t)$ is the enrichment at time t in an ISS with environmental conditions (Eqn 4), $\delta^{18}O_{NSS}(t-\Delta t)$ is the NSS enrichment at the previous time step, and Δt is the interval between time steps (usually 20 min). NSS calculations were initialized with $\delta^{18}O_{ISS}$ values on the preceding day at 1600 when NSS and ISS predictions were usually closest. The leaf water turnover time is defined as: $\tau = V/(gw_i)$, with leaf water volume (V, mol m^{-2}) and conductance to water vapour (g, mol m^{-2} s^{-1}) combining boundary layer and stomatal components. We estimated V (11.8 ± 0.7 mol m^{-2}, no clear diurnal cycle) from the difference between fresh and dry weight (FW and DW, respectively) of 18 needle samples with respect to the projected leaf areas. Equation 5 is an analytical solution of the differential equation given by Cernusak *et al.* (2002) assuming constant V (derivation given in Appendix A). Under this condition, the equation is easier to apply because it does not require iterative solution.

RESULTS

Field observations

Diurnal patterns of branch gas exchange

During 18/19 May and 20 July 2001, we measured photon flux density, relative humidity, temperatures and CO_2 mole fraction in branch chambers containing Sitka spruce branches. The chambers were closed for 5 min each on an automated 20 min cycle. From the changes in CO_2 and water mole fractions monitored every 5 s during chamber closure, we calculated g_s (Fig. 1b) for each closure period and A (Fig. 1a), and all other variables (C_c, $\bar{a}$, etc.) for each 5 s time step within a closure period. When direct g_s data was not available because of high humidity at night, the average observed nocturnal g_s (0.022 mol m^{-2} s^{-1}) was used in the calculations. Further diurnal environmental and gas exchange data are presented in Wingate (2003).

Diurnal $^{18}\Delta$

We determined a total of 29 values of $^{18}\Delta_{A,obs}$ and $^{18}\Delta_{R,obs}$ from flask sample pairs (Eqn 1). The observed values showed pronounced diurnal variability (Fig. 2). The extremely high dawn and dusk $^{18}\Delta_{A,obs}$ values (≈ 100‰) were in sharp contrast to those during the morning (≈ 10‰) and afternoon (20–60‰). The highest day-time value (126‰) was measured in the mid canopy at noon in May. This and the high dusk and dawn values coincided with low net fluxes (Fig. 1). Extremely large $^{18}\Delta_{R,obs}$ values were also observed at night (up to −260‰). Note that negative $^{18}\Delta_{R,obs}$ values

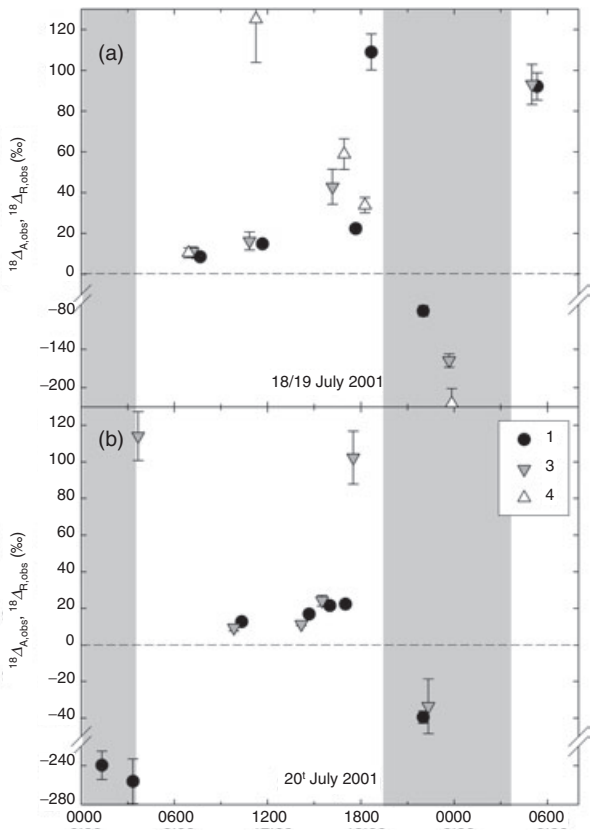

Figure 2. Diurnal variation in observed ^{18}O discrimination during photosynthesis ($^{18}\Delta_{A,obs}$) and nocturnal respiration ($^{18}\Delta_{R,obs}$) of foliage in the upper (1, ●; 3, ▼) and middle (4, △) branch chambers measured on (a) 18/19 May and (b) 20 July 2001. Error bars represent estimated uncertainties (see Methods).

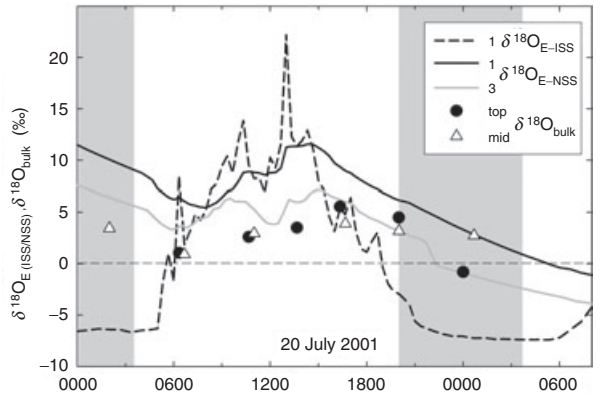

Figure 3. Diurnal variation in predicted $\delta^{18}O_E$ of evaporating site water assuming isotopic steady state ($\delta^{18}O_{E–ISS}$, – – –) and non-steady state ($\delta^{18}O_{E–NSS}$, —) for foliage in the upper branch chambers (1, black; 3, grey, only NSS) and observed bulk water $\delta^{18}O$ of needle samples ($\delta^{18}O_{bulk}$) collected at the top (●) and middle (△) of the canopy on 20 July 2001.

mean that the nocturnal foliage isoflux has a positive sign, i.e. the nocturnal gas exchange results in the ^{18}O enrichment of canopy CO_2 like the day-time gas exchange.

The $\delta^{18}O$ signatures of bulk needle, twig and soil water

Direct sampling of leaf water within the chambers would have been destructive and was not considered an option in our experiments. Instead, we collected needle samples from adjacent trees during the field campaigns (Fig. 3). The average bulk water $\delta^{18}O$ from twig samples (Table 1) were used to define the source water composition $\delta^{18}O_S$ (Eqn 4). Efforts to measure water vapour $\delta^{18}O$ proved unsuccessful for this study. The water vapour composition $\delta^{18}O_V$ was assumed to reflect isotopic equilibrium with that of precipitation from recent rain events, captured in water samples from the soil surface, $\delta^{18}O_{SW}$ (Table 1). The $\delta^{18}O$ signatures of bulk needle water had only small diurnal variations (5–8‰). The difference between needle and twig water $\delta^{18}O$ was large and surprisingly stable (≈ 10‰), even at night. These differences were established over small distances as twigs and needles were usually sampled together, i.e. the attached needles were separated from the respective twigs.

Simulations

Predictions of the $\delta^{18}O$ signature of evaporating site water

Compared with controlled laboratory experiments, plants in the field usually experience fluctuating environmental conditions. Thus, their foliage water may rarely reach ISS, the fundamental assumption of the Craig & Gordon (1965) model normally used to predict the $\delta^{18}O$ composition of leaf water. To examine the role of NSS effects, the $\delta^{18}O$ signature of evaporating site foliage water was calculated on the basis of the chamber measurements (g_s, etc.) and water $\delta^{18}O$ data (Table 1) for each closure period assuming steady state ($\delta^{18}O_{ISS}$, Eqn 4) and NSS ($\delta^{18}O_{NSS}$, Eqn 5) conditions. Typical maximum $\delta^{18}O_{NSS}$ values were ≈ 5‰ lower and shifted towards the afternoon compared with those of $\delta^{18}O_{ISS}$ (Fig. 3). In July, changes in environmental conditions were gradual, with a clear maximum of predicted $\delta^{18}O_{ISS}$ at noon. The May sampling day (not shown) had more fluctuations in $\delta^{18}O_{ISS}$ on timescales of around 1 h as a result of rapid changes in cloud cover. These were effectively smoothed in $\delta^{18}O_{NSS}$ because of the dependency of NSS enrichment on leaf water turnover. In both months, predicted $\delta^{18}O_{ISS}$ values increased rapidly by 5–10‰ within 1–2 h after dawn, whereas increases in $\delta^{18}O_{NSS}$ were much smaller as a result of the low transpiration rates usually found in the morning. On the other hand, $\delta^{18}O_{NSS}$ stayed at a higher level of enrichment in the evening and during the night when $\delta^{18}O_{ISS}$ decreased in the absence of evaporative enrichment. Thus, predicted $\delta^{18}O_{NSS}$ started rising from already enriched signatures compared with $\delta^{18}O_{ISS}$ at dawn.

Predictions of $^{18}\Delta$ during foliage gas exchange

With the chamber gas exchange data (A, C_c, etc.) and $\delta^{18}O_{ISS}$ or $\delta^{18}O_{NSS}$, we predicted the foliage $^{18}\Delta_A$ (Eqn 2) and $^{18}\Delta_{R,bi}$ (Eqn 2), and the (now obsolete) $^{18}\Delta_{R,net}$ (Eqn 3) for each 5 s time step as described in Appendix B. We also calculated the isotopic signature of chamber air ($\delta^{18}O_a$) on the same time step. The $\delta^{18}O_a$ values were initialized with constant $\delta^{18}O_a$ corresponding to their averages from open branch chamber data (Table 1). For the flask sampling periods, we used the $\delta^{18}O_a$ observed in the open branch chambers. We produced two sets of data: One consisted of data at the beginning of closure periods, thus corresponding more closely to the conditions of branches in the absence of chambers. These starting time values of $^{18}\Delta$ (lines in Fig. 4) were used for scaling branch data to the ecosystem (Tables 1 & 2), but they are not exactly comparable to $^{18}\Delta$ measured using the flask samples of chamber air (symbols in Figs 3 & 4). Therefore, we calculated a second set of

Table 1. Average values of parameters used in the simulation of $\delta^{18}O_E$ and ^{18}O discrimination ($^{18}\Delta$) for 18/19 May and 20 July 2001: day-time canopy air temperatures, the $\delta^{18}O$ values of bulk twig and soil water samples, the $\delta^{18}O$ composition of canopy water vapour estimated from soil water $\delta^{18}O$, the isotopic composition of canopy CO_2, $\delta^{18}O_a$ and the flux-weighted diffusional fractionation, $\bar{a}$, for the upper (u) and middle (m) branch chambers

Daily average values of:	18/19 May 2001	20 July 2001
Day-time canopy air temperature	9 °C	12 °C
Twig bulk water $\delta^{18}O$	–7.9 ± 1.6‰	–6.9 ± 0.4‰
Soil bulk water $\delta^{18}O_{SW}$	–6.9 ± 1.5‰	–8.5 ± 0.7‰
Water vapour $\delta^{18}O$, $\delta^{18}O_V$	–17.8‰	–18.4‰
Day-time $\delta^{18}O_a$ of canopy CO_2	1.3 ± 0.1‰	0.9 ± 0.1‰
Diffusional fractionation, $\bar{a}$	7.3‰ (u), 6.2‰ (m)	6.7‰ (u)

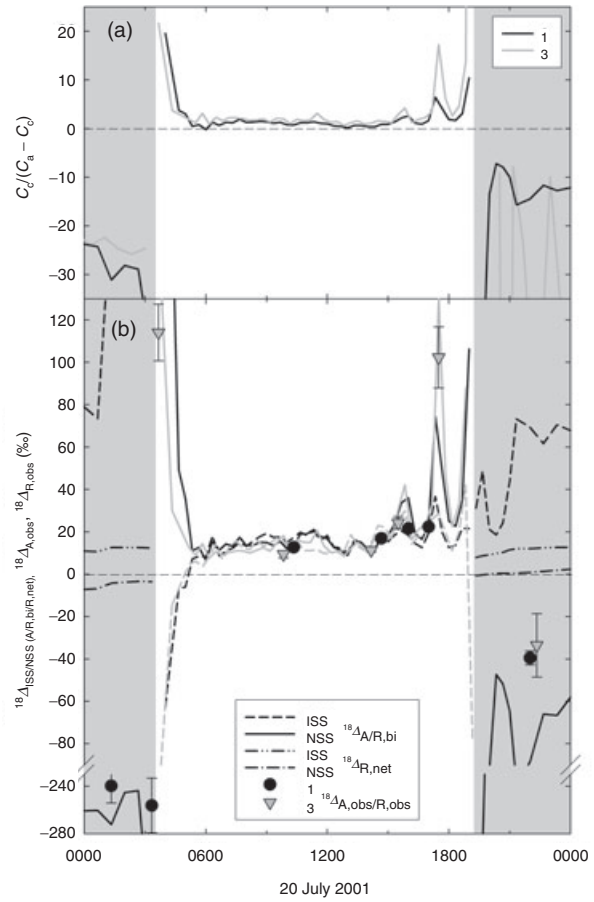

Figure 4. Diurnal variation in (a) $C_c/(C_a - C_c)$ and (b) values of ^{18}O discrimination during photosynthesis ($^{18}\Delta_A$) and nocturnal respiration, ($^{18}\Delta_{R,bi}$ and $^{18}\Delta_{R,net}$) predicted from chamber gas exchange data for the upper branch chambers (1, black; 3, grey) on 20 July 2001. Also shown are the observed values of ^{18}O discrimination during photosynthesis ($^{18}\Delta_{A,obs}$) and nocturnal respiration ($^{18}\Delta_{R,obs}$) (1, ●; 3, ▼). The $^{18}\Delta_A$ and $^{18}\Delta_{R,bi}$ values (Eqn 2) were calculated assuming isotopic steady state (ISS, – – –) and non-steady state (NSS, —) enrichment of evaporating site foliage water. Values predicted from the (now obsolete) net-flux description, $^{18}\Delta_{R,net}$ (Eqn 3), are also shown (ISS, –··–··–; NSS, –·–·–). To improve clarity, only the results for chamber 1 (black) and the $^{18}\Delta_A$ values for chamber 3 (grey) are shown in panel (b).

integrated $^{18}\Delta$ by simulating the flask filling during the chamber closure periods (Appendix B). By incorporating the feedbacks of changing chamber conditions on isotopic gas exchange as captured in the flask samples, this set of $^{18}\Delta$ predicted from gas exchange measurements could then be quantitatively compared with flask $^{18}\Delta_{obs}$ data (Fig. 5). To illustrate the importance of integrating values over the chamber closure periods (Appendix B), the integrated $^{18}\Delta_{R,bi}$ values for 20 July, 2001 were 50 and –65‰ (ISS and NSS, respectively), less extreme than the starting time values of 69 and –88‰ (ISS and NSS, respectively).

The diurnal curves of $^{18}\Delta$ predictions using $\delta^{18}O_{NSS}$ ($^{18}\Delta_{NSS}$) closely followed that of the ratio of retroflux to net uptake of CO_2 [$C_c/(C_a - C_c)$, Fig. 4a], whereas the diurnal

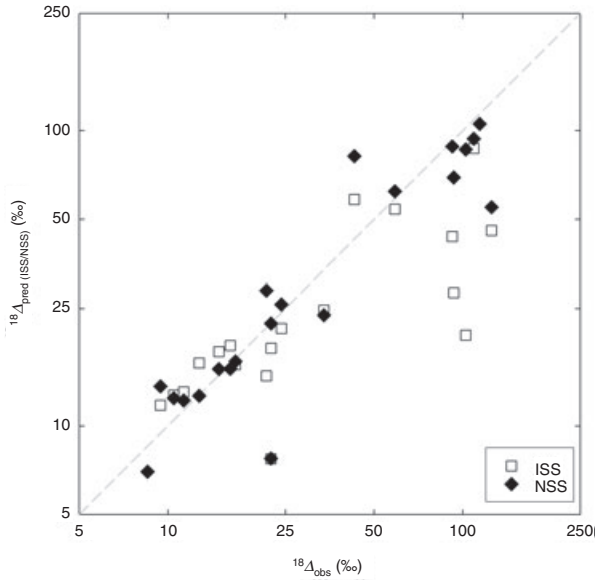

Figure 5. Relationship between predicted and observed ^{18}O discrimination ($^{18}\Delta_{pred}$ and $^{18}\Delta_{obs}$, respectively) for foliage in the branch chambers on 18/19 May and 20 July 2001. Values of $^{18}\Delta$ were predicted assuming isotopic steady state (ISS, □) and non-steady state (NSS, ◆) for the ^{18}O enrichment of evaporating site foliage water. Both axes are on a logarithmic scale.

Table 2. Daily foliage isofluxes (= $^{18}\Delta \times$ flux, per m^2 ground area) estimated from branch chamber gas exchange data (time step, 20 min) integrated over 24 h for 19 May (upper rows) and 20 July (lower rows) 2001. The $\delta^{18}O$ signatures of evaporating site foliage water were calculated in isotopic steady state (ISS) and non-steady state (NSS) versions. Net canopy isofluxes ($\Delta_N F_N$, foliage only) reflect combinations of day-time photosynthetic ($\Delta_A F_A$) and nocturnal respiratory ($\Delta_R F_R$) isofluxes. Net canopy and nocturnal respiration isofluxes are based on either the net-flux ($\Delta_{R,net}$, Eqn 3) or bidirectional ($\Delta_{R,bi}$, Eqn 2) approaches to nocturnal foliage gas exchange

	ISS isofluxes (‰ mol m^{-2} d^{-1})			NSS isofluxes (‰ mol m^{-2} d^{-1})		
		$\Delta_N F_N$ Eqn 3 (net)	$\Delta_N F_N$ Eqn 2 (bi)		$\Delta_N F_N$ Eqn 3 (net)	$\Delta_N F_N$ Eqn 2 (bi)
19 May		**19.3**	**19.3**		**22.0**	**27.4**
20 July		**14.7**	**11.7**		**17.2**	**20.2**
	$\Delta_A F_A$ Eqn 2 (bi)	$\Delta_R F_R$ Eqn 3 (net)	$\Delta_R F_R$ Eqn 2 (bi)	$\Delta_A F_A$ Eqn 2 (bi)	$\Delta_R F_R$ Eqn 3 (net)	$\Delta_R F_R$ Eqn 2 (bi)
19 May	19.9	–0.6	–0.6	21.9	0.1	5.5
20 July	15.0	–0.3	–3.3	17.2	0.0	3.0

$^{18}\Delta_{ISS}$ curves show the opposite pattern because of their negative values in the morning, evening and at night (Fig. 4b). Note that the change in sign between day and night $^{18}\Delta_{NSS}$ is a result of the change in sign of the net CO_2 flux. During the majority of the day (≈ 0600–1500), the differences between $^{18}\Delta_{A,ISS}$ and $^{18}\Delta_{A,NSS}$ were small (1–2‰). In contrast, they differed by 40–200‰ at dawn, dusk and during the night.

Comparison of simulations and observations

The bulk water $\delta^{18}O$ data were in better agreement with the $\delta^{18}O_{NSS}$ values than with those assuming steady state, $\delta^{18}O_{ISS}$, especially in the evenings and at night (Fig. 3). The $\delta^{18}O_{NSS}$ values had small diurnal variations (≈ 10‰) similar to those of bulk water $\delta^{18}O$ data (5–8‰), whereas the steady state predicted $\delta^{18}O_{ISS}$ had much larger diurnal variations (≈ 20‰). Bulk water $\delta^{18}O$ data were generally lower than evaporating site water $\delta^{18}O$ values, as expected because of the Péclet effect (Farquhar & Lloyd 1993; Barbour & Farquhar 2003). A more quantitative comparison between bulk and evaporating site $\delta^{18}O$ values was not possible as the needle samples for bulk water analyses were collected outside the chambers.

The prediction, $^{18}\Delta_{NSS}$, were generally in better agreement with $^{18}\Delta_{obs}$ than those assuming an ISS, $^{18}\Delta_{ISS}$ (Fig. 4b). During the day, this was most obvious at dusk, dawn and in the late afternoon, when only the $^{18}\Delta_{NSS}$ predictions accounted for both the magnitude and sign of $^{18}\Delta_{A,obs}$. The consequences of NSS effects were even more pronounced at night. Clearly, the NSS approach combined with the bidirectional formulation of nocturnal foliage gas exchange ($^{18}\Delta_{R,bi}$, Eqn 2) was required to account for the large negative $^{18}\Delta_{R,obs}$ values found at night. In most cases, the steady state assumption did not even predict the sign of the observed $^{18}\Delta_{R,obs}$ correctly. For example, the integrated values of 50 and –65‰ (ISS and NSS, respectively) for $^{18}\Delta_{R,bi}$ can be compared with the $^{18}\Delta_{R,obs}$ value of –40‰ (20 July, 2001). At the same time, the previously used net flux description ($^{18}\Delta_{R,net}$, Eqn 3) predicted much smaller values, 12 and 1‰ (ISS and NSS, respectively), and thus failed to account for the magnitude of the observed values.

The combined observations from all sampling campaigns were compared with the $^{18}\Delta_{pred}$ in Fig. 5. Dawn and dusk samples ($^{18}\Delta_{A,obs}$ of 92–126‰) were representative for less than 10% of the photosynthetic period but constituted almost one-third of all samples because of our sampling strategy. To reduce any bias introduced by this, the correlation parameters and SEs of $^{18}\Delta_{pred}$ versus $^{18}\Delta_{obs}$ were obtained using the least absolute deviations method. We found the $^{18}\Delta_{pred}$ assuming NSS enrichment of foliage water at the evaporating sites in better agreement with the observations ($^{18}\Delta_{NSS}$, slope: 0.81 ± 0.13, intercept: 3.6 ± 9.5, R^2: 0.74) than predictions assuming an ISS ($^{18}\Delta_{ISS}$, slope: 0.26 ± 0.15, intercept: 12.0 ± 7.8, R^2: 0.45).

Daily foliage isofluxes

The daily canopy isofluxes (= $^{18}\Delta \times$ flux, foliage only) were estimated by integrating chamber flux measurements and their calculated $^{18}\Delta$ values over 24 h (Table 2). The canopy isoflux ($\Delta_N F_N$) combines those of day-time photosynthesis ($\Delta_A F_A$) and nocturnal respiration ($\Delta_R F_R$, $\Delta_{R,bi/net}$ from Eqn 2 or 3). For our field days, assuming ISS would result in underestimation of net canopy isofluxes by ≈ 30% when combined with the bidirectional version of nocturnal foliage gas exchange. Approximately half of that occurs due to NSS-related changes in $\delta^{18}O_E$, i.e. the difference between negative $\delta^{18}O_{ISS}$ and positive $\delta^{18}O_{NSS}$ values, particularly at night (Fig. 3); the other half is caused by bidirectional exchange-related amplification of $^{18}\Delta_R$, i.e. the difference between Eqns 2 and 3.

DISCUSSION

Diurnal $^{18}\Delta$

This study aims to provide an evaluation of the steady state and NSS models of foliage water ^{18}O enrichment under field conditions. We assumed that the discrimination theory (Farquhar & Lloyd 1993) would capture the variability of photosynthetic and respiratory $^{18}\Delta$ values in the field, given measurements of the CO_2 and water mole fractions and flux rates and estimates of the ^{18}O enrichment of water at the evaporating sites of foliage. By comparing $^{18}\Delta$ predictions based on the two enrichment models with flask observed values of $^{18}\Delta$, we tested how important NSS effects on foliage water $\delta^{18}O$ are in shaping the diurnal patterns of $\delta^{18}O$ signatures of foliage CO_2 fluxes.

We found that foliage $^{18}\Delta$ was determined by the interplay of three related factors: the ratio of retrodiffusion to net flux of CO_2 $[C_c/(C_a - C_c)]$, the NSS effects of foliage water turnover on the ^{18}O enrichment of evaporating site water, and the effects of nocturnal g_s on the isotopic exchange of CO_2 and water between the foliage and canopy air at night. The main results of this study were (1) the direct observational evidence for NSS effects; (2) the extremely high apparent $^{18}\Delta$ values in the morning, evening and at night; and (3) the persistently enriched $\delta^{18}O$ values of bulk leaf water at night. We found that the NSS approach (Dongmann *et al.* 1974) substantially improved the agreement between $^{18}\Delta_{pred}$ and $^{18}\Delta_{obs}$ (Fig. 5) compared with the ISS assumption (Craig & Gordon 1965) for the $\delta^{18}O$ signature of evaporating site water.

The relative humidity of canopy air controls $^{18}\Delta$ through both the steady state level of foliage water enrichment and g_s, which limits the rate of CO_2 retrodiffusion and the approach to steady state (Eqn 5). While steady state foliage water enrichment could be calculated without g_s data, measurements of g_s during the day and at night now turn out to be crucial in estimating NSS foliage water ^{18}O enrichment and thus the isotopic impact of foliage gas exchange on atmospheric CO_2. On the diurnal timescale, the retrodiffusion ratio was more important in determining the shape of the $^{18}\Delta$ curve (Fig. 4) than variations in leaf water enrich-

Table 3. Daily flux weighted values of photosynthetic ^{18}O discrimination ($^{18}\Delta$) (Eqn 2) for 19 May and 20 July 2001 assuming isotopic steady state ($^{18}\Delta_{ISS}$) or non-steady state ($^{18}\Delta_{NSS}$) for the enrichment of water at the evaporating sites of foliage

Mean $^{18}\Delta_A$ (‰)	Chamber	$^{18}\Delta_{ISS}$	$^{18}\Delta_{NSS}$	Difference
19 May 2001	1	17.8	19.7	1.9
	3	34.6	39.5	4.9
	4	24.9	25.8	0.9
	all	**25.8**	**28.3**	**2.5**
20 July 2001	1	15.6	17.4	1.8
	3	13.6	15.2	1.6
	all	**14.6**	**16.3**	**1.7**

ment. Thus, diurnal variations in the retrodiffusion ratio need to be considered, for example, in ecosystem scale studies. On the longer timescales relevant for global scale studies, leaf water enrichment played a bigger role. For example, the daily mean photosynthetic $^{18}\Delta_A$ values (Table 3) were 12‰ smaller in July, when both CO_2 and water fluxes were lower, compared with May, with the effects of less enriched leaf water outweighing those of lower internal CO_2 gradients. For both months, our estimates of daily mean $^{18}\Delta_A$ were 2–3‰ higher when taking NSS effects into account (Table 3) because of the higher levels of enrichment at the evaporating sites already present in the mornings. Firstly, this indicates that the isotopic exchange between enriched leaf water and depleted canopy water vapour, scaled by g_s, can be slow enough to cause needle water $\delta^{18}O$ values to stay enriched until morning. Consistent with the nocturnal stomatal exchange, Grace, Malcolm & Bradbury (1975) reported that the stomata of Sitka spruce needles were open in the dark at high relative humidity. Secondly, this and the large difference between needle and twig water $\delta^{18}O$ at night also indicate that the bulk needle water does not return to the depleted $\delta^{18}O_S$ at night, consistent with a large longitudinal Péclet number (Farquhar & Gan 2003).

Experimental caveats

The biggest uncertainty in the simulations of $\delta^{18}O_E$ and $^{18}\Delta$ was probably introduced by the lack of canopy water vapour $\delta^{18}O$ measurements because of technical difficulties during the collection of water vapour samples. To illustrate this, we calculated that a 1‰ shift in $\delta^{18}O_V$ would lead to errors of ≈ 0.4‰ in $\delta^{18}O_E$, and ≈ 0.9‰ at dawn and dusk. Diurnal variations in $\delta^{18}O_V$ have been mainly attributed to transpiration fluxes (Harwood *et al*. 1999) which were small in this study. Nevertheless, $\delta^{18}O_V$ is an important variable and attempts to collect $\delta^{18}O_V$ data should be made in future studies. Gradients in leaf water $\delta^{18}O_E$ along the needles should not affect the (whole-leaf integrated) $^{18}\Delta$ under steady and approximately uniform gas exchange conditions (Farquhar & Gan 2003). It has also been shown that $\delta^{18}O_{NSS}$ calculations are not sensitive to variations in V (Farquhar & Cernusak 2005). Control measurements using an empty chamber confirmed that the isotopic exchange between CO_2 and water was not affected by condensation in the chambers or sampling lines.

Other, minor caveats include the contributions of woody tissue to the net and isotopic gas exchange of CO_2 and water. We estimated typical bark fluxes in the order of 1–5% of foliage fluxes at low light, and even less during the rest of the day. Lastly, if the carbonic anhydrase catalysed isotopic exchange between CO_2 and leaf water is incomplete, using Eqn 2 leads to an overestimation of $^{18}\Delta$ (Farquhar & Lloyd 1993). For coniferous trees, isotopic exchange has been assumed very close to complete (Wang *et al*. 1998). To illustrate how a potentially incomplete isotopic exchange would affect $^{18}\Delta$, we calculate that applying a coefficient (θ) of 0.9 would decrease $^{18}\Delta$ by 1–2‰ (Gillon & Yakir 2000) compared with full isotopic equilibrium of CO_2.

Canopy isofluxes and implications for models

Because the steady state equation tends to overpredict the foliage water ^{18}O enrichment in the morning and to underpredict it in the afternoon, it could be argued that the errors associated with NSS effects might cancel over the course of the day. This was not the case in this study. As the higher levels of enrichment reached in the afternoon persisted through the night, the nocturnal foliage gas exchange contributed substantially to the increase in the net isoflux (Table 2). We expect these effects to be large under conditions of high relative humidity, for species with high specific leaf water content, and when stomata are open at night. This might occur in boreal and tropical forests, but also in all other types of ecosystems during times of high relative humidity. Thus, the two effects described here, NSS-related changes in leaf water $\delta^{18}O_E$ and bidirectional exchange-related amplification of $^{18}\Delta_R$, both have important implications for global modelling (Farquhar *et al*. 1993; Ciais *et al*. 1997a, Cuntz *et al*. 2003a) and for the interpretation of field measurements of the $\delta^{18}O$ of CO_2 (Bowling *et al*. 2003; Ometto *et al*. 2005). In the context of bidirectional exchange, the feedbacks between foliage $^{18}\Delta$ and the $\delta^{18}O$ of canopy CO_2 (Eqn 2) also become important, particularly at night. We suggest that NSS effects and the explicit description of an interactive canopy air space should be included in ecosystem or global studies using the $\delta^{18}O$ signatures of CO_2.

CONCLUSIONS

We observed pronounced diurnal variations in $^{18}\Delta_A$ and $^{18}\Delta_R$ by Sitka spruce branches in branch chambers deployed in the field. We used the ISS and NSS models of foliage water ^{18}O enrichment to estimate $^{18}\Delta$ based on the theoretical approach of Farquhar & Lloyd (1993), and compared these estimates with the field observations. Predictions of $^{18}\Delta$ assuming ISS did not agree well with our data at most times, highlighting the limitations of the Craig & Gordon (1965) model widely used in numerical models. Taking the gradual development of ^{18}O enrichment throughout the day into account (Dongmann *et al*. 1974) substantially improved the agreement between $^{18}\Delta_{pred}$ and $^{18}\Delta_{obs}$. The direct observa-

tional evidence for NSS effects in this study comprises, firstly, the extremely high apparent signatures of CO_2 fluxes ($^{18}\Delta_{A/R,obs}$) in the morning, evening and at night, and secondly, the small diurnal amplitude and enriched night-time values of bulk needle water $\delta^{18}O$. We conclude that NSS effects on foliage water enrichment can play an important role in determining the $\delta^{18}O$ signatures of photosynthetic and respiratory CO_2 exchange between foliage and canopy air. NSS effects are probably most pronounced in species with low transpiration rates or with high specific leaf water content such as conifers, and when stomata are open at night or when there is high relative humidity. This might apply, for example, to large parts of boreal ecosystems and thus plays a role in shaping the interhemispheric gradient in $\delta^{18}O$ of CO_2. It is therefore important to include NSS effects in global simulations of the $\delta^{18}O$ of atmospheric CO_2.

ACKNOWLEDGMENTS

We wish to thank H. Geilmann, A. Jordan, M. Rothe and R. Werner for carrying out the analyses of air and organic samples at the MPI für Biogeochemie in Jena, Germany; N. Betson, G. Lanigan and H. Griffiths for analyses of water samples in Cambridge, UK; and D. Hemming and D. Yakir for extractions and analyses of water samples in Rehovot, Israel. We thank R. Clement, V. Finlayson, S. Patiño, F. Ripullone, J. Schmerler and A. Zerva for help in the field. We are grateful to W. Brand and M. Cuntz for advice, to S.C. Wong and J. Severinghaus for loan of equipment, and to M. Heimann for continued support and discussions. We also thank D. Yakir and the anonymous reviewers for their valuable comments. This work was partly supported by a Marie Curie International Fellowship to US (MOIF-CT-2004-2704) and a Natural Environment Research Council Studentship to LW (GT04/98/93/TS).

REFERENCES

Barbour M.M. & Farquhar G.D. (2003) Do pathways of water movement and leaf anatomical dimensions allow development of gradients in $H_2{}^{18}O$ between veins and the sites of evaporation within leaves? *Plant, Cell and Environment* **27,** 107–121.

Bariac T., Gonzalez-Dunia J., Katerji N., Bithenod O., Bertolini J.M. & Mariotti A. (1994) Variabilité spatio-temporelle de la composition isotopique de l'eau (^{18}O, ^{2}H) dans le continuum sol-plante-atmosphère 2. Approche en conditions naturelles. *Chemical Geology* **115,** 317–333.

Bowling D.R., McDowell N.G., Welker J.M., Bond B.J., Law B.E. & Ehleringer J.R. (2003) Oxygen isotope content of CO_2 in nocturnal ecosystem respiration: 2. Short-term dynamics of foliar and soil component fluxes in an old-growth ponderosa pine forest. *Global Biogeochemical Cycles* **17**, doi 10.1029/2003GB002082, 1–12.

Brenninkmeijer C.A.M., Kraft P. & Mook W.G. (1983) Oxygen isotope fractionation between CO_2 and H_2O. *Isotope Geoscience* **1,** 181–190.

Cappa C.D., Hendricks M.B., DePaulo D.J. & Cohen R.C. (2003) Isotopic fractionation of water during evaporation. *Journal of Geophysical Research* **108,** 4525–4534.

Cernusak L.A., Pate J.S. & Farquhar G.D. (2002) Diurnal variation in the stable isotope composition of water and dry matter in fruiting *Lupinus angustifolius* under field conditions. *Plant, Cell and Environment* **25,** 893–907.

Cernusak L.A., Wong S.C. & Farquhar G.D. (2003) Oxygen isotope composition of phloem sap in relation to leaf water in *Ricinus communis*. *Functional Plant Biology* **30,** 1059–1070.

Cernusak L.A., Farquhar G.D., Wong S.C. & Stuart-Williams H. (2004) Measurement and interpretation of the oxygen isotope composition of carbon dioxide respired by leaves in the dark. *Plant Physiology* **136,** 3350–3363.

Cernusak L.A., Farquhar G.D. & Pate J.S. (2005) Environmental and physiological controls over oxygen and carbon isotope composition of Tasmanian blue gum, *Eucalyptus globulus*. *Tree Physiology* **25,** 129–146.

Ciais P., Denning A.S., Tans P.P., *et al.* (1997a) A three-dimensional synthesis study of $\delta^{18}O$ in atmospheric CO_2. 1. Surface fluxes. *Journal of Geophysical Research* **102,** 5857–5872.

Ciais P., Tans P.P., Denning A.S., *et al.* (1997b) A three-dimensional synthesis study of $\delta^{18}O$ in atmospheric CO_2. 2. Simulations with the TM2 transport model. *Journal of Geophysical Research* **102,** 5873–5883.

Craig H. & Gordon L. (1965) Deuterium and Oxygen-18 Variation in the Ocean and the Marine Atmosphere, in: *Stable Isotopes in Oceanography Studies and Paleotemperatures*Laboratory of Geology and Nuclear Science, Pisa, Italy. pp. 9–130.

Cuntz M., Ciais P., Hoffmann G., Allison C.E., Francey R., Knorr W., Tans P.P., White J.W.C. & Levin I. (2003a) A comprehensive global three-dimensional model of $\delta^{18}O$ in atmospheric CO_2 2. Mapping the atmospheric signal. *Journal of Geophysical Research* **108**, doi 10.1029/2002JD003154, 1–24.

Cuntz M., Ciais P., Hoffmann G. & Knorr W. (2003b) A comprehensive global three-dimensional model of $\delta^{18}O$ in atmospheric CO_2 1. Evaluation of surface fluxes, *Journal of Geophysical Research* **108**, doi 10.1029/2002JD003153, 1–19.

Dongmann G., Nürnberg H.W., Förstel H. & Wagener K. (1974) Enrichment of $H_2{}^{18}O$ in leaves of transpiring plants. *Radiation and Environmental Biophysics* **11,** 41–52.

Farquhar G.D. & Cernusak L.A. (2005) On the isotopic composition of leaf water in the non-steady state. *Functional Plant Biology* **32,** 293–303.

Farquhar G.D. & Gan K.S. (2003) On the progressive enrichment of the oxygen isotopic composition of water along a leaf. *Plant, Cell and Environment* **26,** 801–819.

Farquhar G.D. & Lloyd J. (1993) Carbon and oxygen isotope effects in the exchange of carbon dioxide between terrestrial plants and the atmosphere. In *Stable Isotopes and Plant Carbon-Water Relations* (eds J.R. Ehleringer, A.E. Hall & G.D. Farquhar) pp. 47–70. Academic Press, NY, USA.

Farquhar G.D., Lloyd J., Taylor J.A., Flanagan L.B., Syvertsen J.P., Hubick K.T., Wong S.C. & Ehleringer J.R. (1993) Vegetation effects on the isotope composition of oxygen in atmospheric CO_2. *Nature* **363,** 439–443.

Francey R.J. & Tans P.P. (1987) Latitudinal variation in ^{18}O of atmospheric CO_2. *Nature* **327,** 495–497.

Gillon J.S. & Yakir D. (2000) Internal conductance to CO_2 diffusion and ($C^{18}OO$) – ^{18}O discrimination in C_3 leaves. *Plant Physiology* **123,** 201–213.

Grace J., Malcolm D.C. & Bradbury I.K. (1975) Effect of wind and humidity on leaf diffusive resistance in Sitka spruce seedlings. *Journal of Applied Ecology* **12,** 931–940.

Guy R.D., Berry J.A., Fogel M.L. & Hoering T.C. (1989) Differential fractionation of oxygen isotopes by cyanide-resistant and cyanide-sensitive respiration in plants. *Planta* **177,** 483–491.

Harwood K.G., Gillon J.S., Griffiths H. & Broadmeadow M.S.J. (1998) Diurnal variation of $\delta^{13}CO_2$, $\delta C^{18}O^{16}O$ and evaporative

site enrichment of $\delta H_2{}^{18}O$ in *Piper aduncum* under field conditions in Trinidad. *Plant, Cell and Environment* **21,** 269–283.
Harwood K.G., Gillon J.S., Roberts A. & Griffiths H. (1999) Determinants of isotopic coupling of CO_2 and water vapour within a *Quercus petraea* forest canopy. *Oecologia* **119,** 109–119.
Jarman P.D. (1974) The diffusion of carbon dioxide and water vapour through stomata. *Journal of Experimental Botany* **25,** 927–936.
Ludlow M.M. & Jarvis P.G. (1971) Photosynthesis in Sitka Spruce [*Picea Sitchensis* (Bong) Carr] 1. General Characteristics. *Journal of Applied Ecology* **8,** 925–953.
Majoube M. (1971) Oxygen-18 and deuterium fractionation between water and steam. *Journal de Chimie Physique et de Physico-Chimie Biologique* **68,** 1423.
Ometto J.P.H., Flanagan L.B., Martinelli L.A. & Ehleringer J.R. (2005) Oxygen isotope ratios of waters and respired CO_2 in Amazonian forest and pasture ecosystems. *Ecological Applications* **15,** 58–70.
Riley W.J., Still C.J., Torn M.S. & Berry J.A. (2002) A mechanistic model of $H_2{}^{18}O$ and $C^{18}OO$ fluxes between ecosystems and the atmosphere: model description and sensitivity analyses. *Global Biogeochemical Cycles* **16**, doi 10.1029/2002GB01878, 1–14.
Seibt U. (2003) Processes controlling the isotopic composition of CO_2 and O_2 in canopy air: a theoretical analysis with some observations in a Sitka spruce plantation. (Thesis). University of Hamburg, Hamburg, Germany.
Wang X.F., Yakir D. & Avishai M. (1998) Non-climatic variations in the oxygen isotopic compositions of plants. *Global Change Biology* **4,** 835–849.
Werner R.A., Rothe M. & Brand W.A. (2001) Extraction of CO_2 from air samples for isotopic analysis and limits to ultra high precision $\delta^{18}O$ determination in CO_2 gas. *Rapid Communications in Mass Spectrometry* **15,** 2152–2167.
Wingate L. (2003) The contribution of photosynthesis and respiration to the net ecosystem exchange and ecosystem ^{13}C discrimination of a Sitka spruce plantation. (Thesis). University of Edinburgh, Edinburgh, UK.
Yakir D. & Wang X.F. (1996) Fluxes of CO_2 and water between terrestrial vegetation and the atmosphere estimated from isotope measurements. *Nature* **380,** 515–517.

Received 3 March 2005; received in revised form 29 July 2005; accepted for publication 28 September 2005

APPENDIX A

Non-steady state (NSS) enrichment for constant leaf water volume (*V*, mol m^{-2})

We consider the isotopic ratio of evaporating site foliage water (R_e) as described for isotopic steady state (ISS) (Craig & Gordon 1965; Farquhar & Gan 2003) and NSS conditions (Dongmann *et al*. 1974; Bariac *et al*. 1994; Farquhar & Cernusak 2005). At constant V (mol m^{-2}), the flux of water into the leaf equals that out of the leaf, i.e. the transpiration rate (E, mol m^{-2} s^{-1}). The isotopic ratio of the flux of water into the leaf (R_s) is assumed to be constant; that of the transpiration flux out of the leaf (R_t) can vary. The change in R_e over time can then be described by (Dongmann *et al*. 1974)

$$V\frac{dR_e}{dt} = R_sE - R_tE. \tag{A1.1}$$

Using $E = g(w_i - w_a)$ and $R_tE = g/\alpha_k(R_ew_i/\alpha_{eq} - R_vw_a)$, the isotope ratio of transpired water, R_t, can be expressed as (e.g. Dongmann *et al*. 1974; Farquhar & Gan 2003)

$$R_t = \frac{1}{\alpha_k}\left(\frac{R_e}{\alpha_{eq}} - R_v\frac{w_a}{w_i}\right)\left(1-\frac{w_a}{w_i}\right)^{-1}. \tag{A1.2}$$

Combining Eqns A1.1 and A1.2 gives a differential equation for R_e:

$$\begin{aligned}\frac{dR_e}{dt} &= \frac{E}{V}(R_s - R_t)\\ &= \frac{E}{V}\left[R_s - \frac{1}{\alpha_k}\left(\frac{R_e}{\alpha_{eq}} - R_v\frac{w_a}{w_i}\right)\left(1-\frac{w_a}{w_i}\right)^{-1}\right],\end{aligned} \tag{A1.3}$$

and defining a turnover time, $\tau = V(1 - w_a/w_i)/E$ [or, since $E = g(w_i - w_a)$, $\tau = V/(gw_i)$], this yields

$$\frac{dR_e}{dt} = \frac{1}{\tau}\frac{1}{\alpha_k\alpha_{eq}}\left[\alpha_k\alpha_{eq}R_s\left(1-\frac{w_a}{w_i}\right) + \alpha_{eq}R_v\frac{w_a}{w_i} - R_e\right]. \tag{A1.4}$$

In the case of ISS, $dR_e/dt = 0$, and Eqn A1.4 is simplified to

$$R_{e,ISS} = \alpha_{eq}\left[\alpha_kR_s\left(1-\frac{w_a}{w_i}\right) + R_v\frac{w_a}{w_i}\right], \tag{A1.5}$$

i.e. the Craig-Gordon equation (Craig & Gordon 1965). If evaporating site enrichment is not at an ISS, but transpiration rate can be assumed constant, then Eqn A1.4 can be solved to give a time-dependent expression for the enrichment:

$$R_e(t) = R_{e,ISS}\left(1 - e^{-\frac{1}{\alpha_k\alpha_{eq}}\frac{t}{\tau}}\right), \tag{A1.6}$$

or integrated over a time step, Δt, in the terms of Eqn 5 of the main text:

$$\begin{aligned}\delta^{18}O_{ISS}(t) - \delta^{18}O_{NSS}(t) = &\left[\delta^{18}O_{ISS}(t) - \delta^{18}O_{NSS}(t-\Delta t)\right]\\ &\cdot e^{-(1-\varepsilon_k)(1-\varepsilon_{eq})\frac{\Delta t}{\tau}}\end{aligned} \tag{A1.7}$$

so that for small Δt or large τ, $e^{-\Delta t/\tau}$ approaches 1 and $\delta^{18}O_{NSS} \approx \delta^{18}O^{t-1}{}_{NSS}$, i.e. no change in leaf water enrichment, and for large Δt or small τ, $e^{-\Delta t/\tau}$ approaches 0 and $\delta^{18}O_{NSS} \approx \delta^{18}O_{ISS}$, i.e. maximum (steady state) leaf water enrichment. Note that permil values such as ε, $\bar{a}$, etc. need to be divided by 1000 when they occur in terms like $(1 - \varepsilon)$ or $(1 - \bar{a})$.

APPENDIX B

Analysis of closed-chamber measurements

Gas exchange in closed chambers will lead to transient changes in microenvironmental conditions, air composition and fluxes during the closure period. Flask samples collected at the beginning and at the end of chamber closure periods integrate over such changes. Also, the air flushed through the flasks and back into the chambers was dried, weakening the increase in chamber water vapour content. We take both into account when comparing flask data with $^{13}\Delta$ and $^{18}\Delta$ predictions based on gas exchange data. Here, we demonstrate how chamber measurements (5 s time step) can be integrated during closure periods to obtain $^{13}\Delta$ and $^{18}\Delta$ predictions directly comparable with observations from the flask sampling system. The quantitative descriptions are based on one example, chamber 1 on 20 July 2001, 1440–1445. The data processing described in the following were implemented in an IDL program.

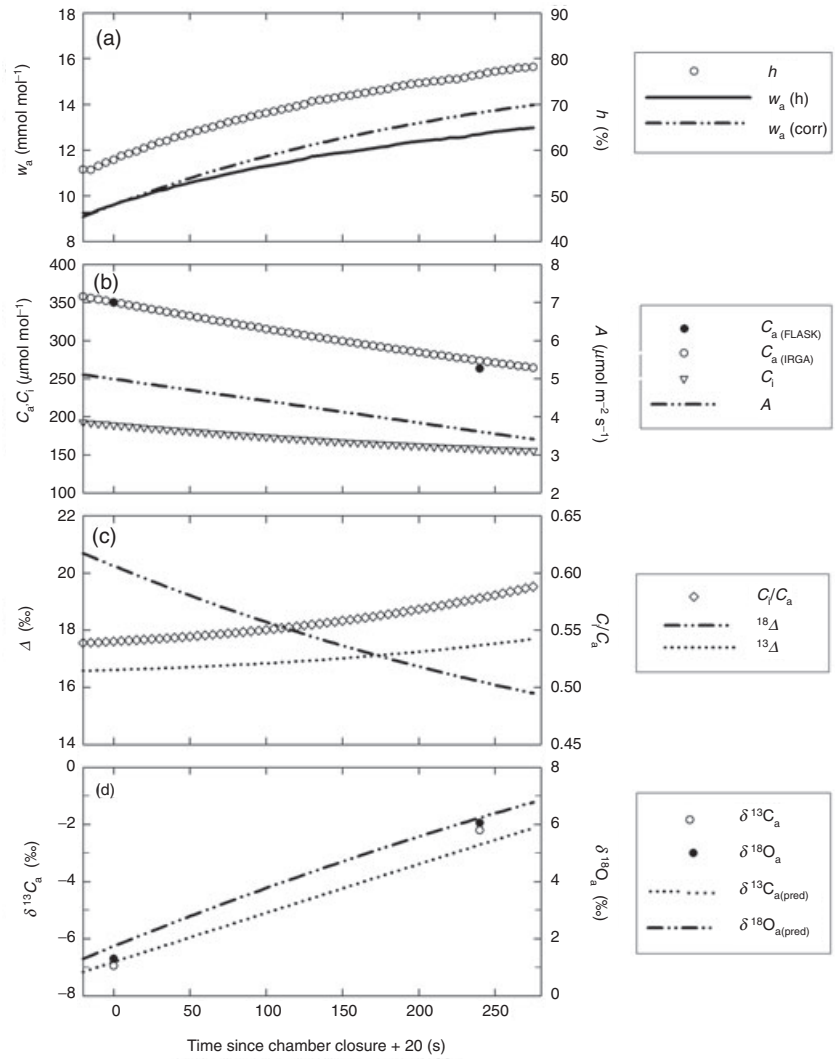

Figure 6. Changes in branch chamber 1 during the 5 min closure period at 1440 on 20 July 2001: (a) observed relative humidity (h) and calculated air vapour mole fraction, uncorrected [$w_{a(h)}$] and corrected [$w_{a(corr)}$] for the recirculation of dried air by the sampling system; (b) CO_2 mole fraction observed by the infrared gas analyser (IRGA) [$C_{a(IRGA)}$] and flask sampling method [$C_{a(FLASK)}$], and calculated intercellular CO_2 mole fraction (C_i) and net assimilation rate (A); (c) calculated ratio of ambient to intercellular CO_2 mole fraction (C_i/C_a) and photosynthetic ^{13}C and ^{18}O discrimination ($^{13}\Delta$, $^{18}\Delta$), and (d) flask observed ($\delta^{13}C_a$, $\delta^{18}O_a$) and calculated [$\delta^{13}C_{a(pred)}$, $\delta^{18}O_{a(pred)}$] isotopic signatures of chamber air.

Photon flux density was fairly stable during chamber closure at 127 ± 3 μmol m^{-2} s^{-1}. Air and leaf temperature were similar at 14 ± 0.7 °C. Stomatal conductance to water vapour (g_s) of *P. sitchensis* has been shown to adjust slowly (up to 45 min) to changes in environmental conditions (Ludlow & Jarvis 1971). Therefore, we assumed that to a good approximation, g_s remained constant during chamber closure (5 min). Preliminary analyses highlighted a lack of sensitivity in our set-up to monitor changes in the H_2O mole fraction using the infrared gas analyser (IRGA). Instead, relative humidity data (h) was used to calculate the vapour mole fraction of the enclosed air [$w_{a(h)}$, Fig. 6a]. During flask sampling periods, the air vapour mole fraction was corrected for the flow of dry air (3 dm^3 min^{-1}) returned from the flask sampling system [$w_{a(corr)}$]. Assuming saturated air at leaf temperature yielded a leaf vapour mole fraction (w_i) of 16.4 mmol mol^{-1}. The total g (0.051 mol m^{-2} s^{-1} for this period) was obtained from the increase in air vapour mole fraction [$w_{a(corr)}$ from 9 to 14 mmol mol^{-1}; h from 56 to 78%] by fitting

$$w_a = w_i + (w_{a0} - w_i)e^{-\frac{L_a}{V_a} g (t - t_0)} \quad \text{(A2.1)}$$

to leaf and air vapour mole fraction data at time t during the closure periods, where w_{a0} is the initial air vapour mole fraction at the starting time t_0. L_a and V_a are the leaf area and air molar volume enclosed in the chamber. The calculated transpiration rate (not shown) decreased from 0.4 to 0.1 mmol m^{-2} s^{-1} with decreasing vapour mole fraction deficit during the closure period. At times of a negative leaf to air mole fraction difference (e.g. at night), the mean value of conductance measured under non-saturated conditions at night was used.

The CO_2 mole fraction of chamber air (C_a, Fig. 6b) decreased from 350 to 275 μmol mol^{-1} over the closure period. We assumed that the concurrent change in the rate of net CO_2 assimilation (A, Fig. 6b) was on the linear part of the CO_2 response curve (Ludlow & Jarvis 1971). The C_a data were fitted with a quadratic equation, its derivative yielding a linear approximation of A (most $R^2 > 0.99$). The decrease in A obtained from changes in C_a (from 5.1 to 3.4 μmol m^{-2} s^{-1}) compared well with that estimated from the normalized slope of the linear part of the CO_2 response curve (from 5.1 to 3.6 μmol m^{-2} s^{-1}). Because C_a and A varied concurrently, the change in the intercellular CO_2 mole

fraction (C_i, Fig. 6b) calculated from A and g incorporating ternary effects (Jarman 1974) was less pronounced than that of C_a, leading to a small increase in C_i/C_a over the closure period (Fig. 6c).

Using the $\delta^{18}O_a$ and $\delta^{13}C_a$ values observed in the open chambers as starting point values, we then calculated $\delta^{18}O_{a(pred)}$ and $\delta^{13}C_{a(pred)}$ (Eqn 1) from $^{18}\Delta$ (Eqn 2) and $^{13}\Delta$ for each time step. The instantaneous $^{13}\Delta$ value increased from 17 to 18‰, whereas that of $^{18}\Delta$ decreased from 21 to 16‰ (Fig. 6c). The calculated $\delta^{13}C_{a(pred)}$ and $\delta^{18}O_{a(pred)}$ increased from –7 to –2‰ and from 1 to 7‰, respectively (Fig. 6d). Weighted averages of $\delta^{13}C_a$, $\delta^{18}O_a$ and C_a corresponding to the mixture of air collected in the 'closed' flask sample were obtained using exponentially increasing weights for data points prior to the pressurizing phase and equal weights thereafter, each contributing half of the air sample, consistent with flask filling tests conducted at the Max Planck Institut (MPI) for Biogeochemistry, Jena, Germany. The integrated $^{13}\Delta$ and $^{18}\Delta$ values were then derived from the $\delta^{13}C_a$, $\delta^{18}O_a$ and C_a at the start, and their weighted averages at the end of chamber closure periods. This approach is equivalent to the calcuations using flask data, making both methods directly comparable. The integrated values were ≈ 0.3‰ higher than starting point values for $^{13}\Delta$ and ≈ 2.1‰ lower for $^{18}\Delta$. For the example used here, the integrated $^{13}\Delta$ and $^{18}\Delta$ values of 16.9 and 19.1‰ were in better agreement with the flask observed values of 17.0 and 16.9‰ than their respective starting point estimates of 16.6 and 21.2‰.

